Biogeochemistry **56:** 311–348, 2001.

Modeling the hydrochemistry of the Choptank River basin using GWLF and Arc/Info: 2. Model Validation and Application

KUANG-YAO LEE[1,2], THOMAS R. FISHER[1] &
EMMA ROCHELLE-NEWALL[1,3]
[1]*Horn Point Laboratory, University of Maryland Center for Environmental Science, P. O. Box 775, Cambridge, MD 21613, U.S.A.;* [2]*Current address: Comprehensive Planning and GIS Support, MD Dept. of Planning, 301 W. Preseton St., Suite 1101, Baltimore, MD 21201-2305, U.S.A.;* [3]*Current address: Observatoire Oceanologique, ESA7076, B.P. 28, Villefranche-sur-Mer, 06234 France*

Key words: Arc/Info, GWLF, hydric soils, nutrients, watershed modeling

Abstract. We used the hydrochemical model GWLF to estimate terrestrial diffuse fluxes from ungauged areas of a coastal plain catchment, the Choptank River basin. The gauged area of the basin is 17% of the land surface, and we divided the remaining ungauged area into 21 sub-basins. Three comparative approaches were used: (1) application of area yield coefficients based on 11 years of observations from the gauged area to extrapolate over ungauged sub-basins without modeling, (2) application of GWLF to estimate export from all sub-basins using model parameters calibrated in the gauged sub-basin, and (3) application of GWLF with parameter adjustments based on the local characteristics in each sub-basin. Comparison of the predicted export from 6 selected sub-basins with observed export data showed that application of GWLF with local adjustments reduced model errors of N export from 43% to 27%. With only one adjustment for sediment P, application of GWLF alone reduced errors of P export from 92% to 40–45%, with or without local adjustments for flow and sediment retention. The data supported the hypothesis that significant spatial variations in N and P yields introduce large errors when extrapolating from gauged to ungauged sub-basins, and estimated TN and TP yield coefficients varied over 1–21 kg N and 0.1–0.5 kg P ha^{-1} y^{-1} in ungauged areas due to varying human population densities, soil drainage characteristics, and amounts of agriculture. The most accurate estimates of terrestrial diffuse sources were combined with point source discharges and wet atmospheric inputs to estimate annual average inputs of 2.5 $\times$ 10^6 kg N and 5.8 $\times$ 10^4 kg P y^{-1} to the Choptank estuary during 1980–1996. These results illustrate the problems of spatial extrapolation from gauged to ungauged areas and emphasize the need for application of local characteristics for accurate assessment of watershed export.

Introduction

The eutrophication of Chesapeake Bay has been caused by the cascading effects of anthropogenic disturbances (Nixon 1987). Increasing human populations have led to intensively managed agriculture and urban land uses; this, in turn, has increased the amount of N and P entering aquatic systems via the atmosphere (Fisher & Oppenheimer 1991), agricultural activities (Beaulac & Reckhow 1982), and sewage discharges (Peierls et al. 1990). The enhanced nutrient inputs have increased the frequency of phytoplankton blooms, augmented organic matter sedimentation rates, and expanded seasonal anoxia in bottom waters (Officer et al. 1984; Malone et al. 1988; Cooper & Brush 1991). These conditions consequently caused habitat degradation for fish and shellfish and a decline in submerged aquatic vegetation (Orth & Moore 1983; Seliger et al. 1985; Stevenson et al. 1993). The cascading effects are due to the strong hydrologic linkages between Chesapeake Bay and its basin.

Anthropogenically disturbed areas (agricultural and urban land uses) have higher nutrient yields (kg N or P ha^{-1} y^{-1}) than forests (e.g. Beaulac & Reckhow 1982). For example, on the coastal plain watersheds of the Chesapeake Bay, Jordan et al. (1997) estimated that N was exported from 100% cropland at a rate of 18 kg N ha^{-1} y^{-1}, 7 times higher than the rate from other land uses. The higher export rates from agricultural areas are the result of lower plant biomass, fertilizer applications, and disturbance. Conversion of forest to agricultural or to urban land uses leads to greater stream flows due to lower evapotranspiration and water interception (Hopkinson & Vallino 1995) as well as increased concentrations of N and P (e.g. Jordan et al. 1997; Norton & Fisher 2000). Therefore, fluxes of N and P (flow $\times$ concentrations) are greatly enhanced in disturbed areas compared to forests.

There is now widespread recognition that high nutrient fluxes from land are a serious environmental problem in many coastal regions. There are several consortia of federal, state, and local agencies which are attempting to reduce inputs of N and P to coastal and estuarine areas from their drainage basins. For instance, in the Chesapeake drainage, a consortium of agencies is attempting to reduce inputs by 40% (Linker 1996; MD DNR 1996), and a 30% target has recently been set for the Mississippi (Arnold et al. 2001).

In order to reduce nutrient inputs to estuaries, a complete understanding of nutrient export from surrounding watersheds is necessary. However, there commonly exist within a watershed ungauged areas discharging unknown quantities of N and P, particularly in coastal plain regions (Gardner et al. 1997). Thus, the total nutrient export for many watersheds is often extrapolated from gauged portions of watersheds using area-normalized yield coefficients (often expressed as kg ha^{-1} y^{-1}). In many basins on Piedmont

and Montaine geological provinces, extrapolation errors may be small (e.g. the Susquehanna River, gauged at Conowingo Dam just before entering Chesapeake Bay). However, smaller coastal plain watersheds often require extrapolation over areas larger than the gauged sites, particularly over areas immediately adjacent to the Bay's shoreline with short hydrologic flow paths. This problem is particularly acute in coastal plain watersheds with low relief and tidal intrusion, and gauged areas often represent <25% of the basin area. For instance, in the Choptank basin, a coastal plain watershed of the Chesapeake drainage on the Delmarva Peninsula, only 17% of the basin is gauged. Direct extrapolation over ungauged areas (83%), using yield coefficients from the gauged watershed, could produce substantial errors because anthropogenic land uses such as agriculture and urban areas may result in large and variable losses of nutrients depending on local conditions such as soil drainage characteristics, topography, land use, etc. (Beaulac & Rechhow 1982; Jordan et al. 1997; Norton & Fisher 2000). Therefore, spatial variations in land use, soils and other characteristics within a basin may introduce significant errors in simple extrapolations of nutrient yields from a gauged sub-basin.

We attempted to address this problem by comparing several approaches to obtain total inputs from the Choptank River basin on the Mid-Atlantic coastal plain. We quantitatively estimated the errors associated with extrapolation from the gauged sub-basin to ungauged areas using three approaches. The goals were (1) to estimate the importance of spatially varying local conditions in determining the fluxes of water, sediment, N, and P in this coastal plain basin and (2) to construct N and P input budgets for the Choptank estuary. The hypothesis that we wished to test was that estimated yield coefficients of N and P from ungauged areas would vary considerably from those of the gauged sub-basin due to spatial variations in land use, soils, and human populations.

Study area

The Choptank basin consists of a land area of 1756 km^2 and an estuary of 280 km^2. The land is located on the Delmarva Peninsula within the Mid-Atlantic coastal plain, and the estuary is a former coastal plain valley flooded after the last glaciation 10,000 years ago. Salinities are as high as 15 psu due to exchange with Chesapeake Bay. On the land surface, agriculture represents 61% of the current land use, 33% is covered by forest, and 5% is urban (Norton & Fisher 2000; Lee et al. 2000). A sub-basin of 294 km^2 has been gauged by USGS since 1948 (Figure 1). This sub-basin represents only 17% of the terrestrial portion of the basin and contains a greater proportion of forest and poorly drained soils (D hydrologic drainage class) than the entire

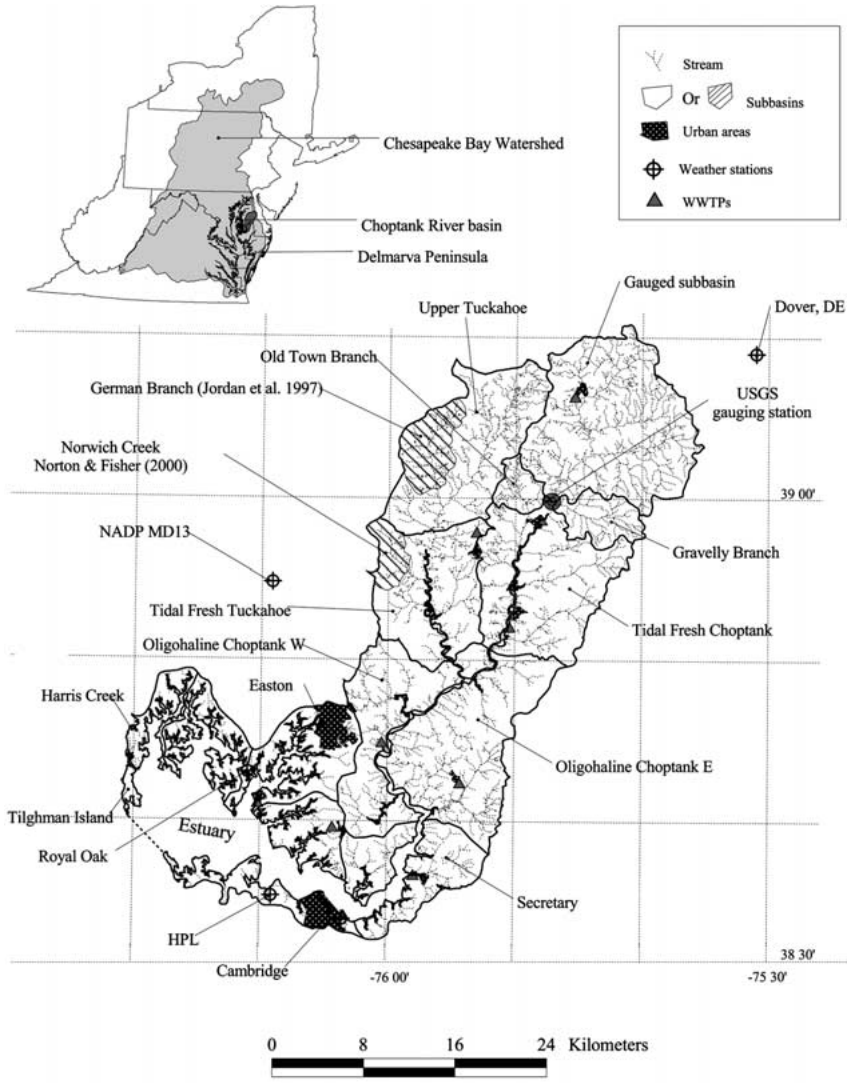

Figure 1. The Choptank River basin on the coastal plain of the Chesapeake Bay drainage. Sub-basins of the Choptank basin (solid lines) were interpreted using hydrogeomorphic properties (Hamilton et al. 1993), previously sampled locations (Jordan et al. 1997; Norton & Fisher 2000), and water quality monitoring stations of the EPA Chesapeake Bay Program (Fisher et al. 1999). Sub-basins include the watershed gauged by USGS (#01491000). Also shown are locations of waste water treatment plants (WWTPs, gray filled triangles) and the urban areas served by each WWTP (hatched areas). The location of atmospheric N deposition stations (NADP MD13 and HPL stations) and weather stations (Royal Oak, Cambridge, and Dover) are shown by cross hair marks. For clarity, some smaller sub-basins listed in Table 1 are not identified.

basin (Lee et al. 2000). Water quality has been monitored since 1964 by USGS (2–30 samples per year, annual USGS water resources data) and since 1979 by our research group (150–200 samples per year, Fisher et al. 1998). In addition, water quality surveys were performed at 35 stream locations in 1985–1986 (Norton & Fisher 2000).

Degraded water quality has been found in waters of the Choptank (MD DNR 1996; Staver et al. 1996). There has been a decline in submerged aquatic vegetation (SAV) due to anthropogenic contributions of diffuse and point source discharges which have enhanced quantities of nutrients in the estuary (MD DNR 1996). The presence of excess nutrients causes enhanced growth of planktonic and periphytic algae which reduce available light for the plants (Stevenson et al. 1993). A better understanding of nutrient inputs to the Choptank from all sources will provide a scientific basis for future nutrient reduction strategies.

Methods

Approaches for estimation of export from ungauged areas

We used a simple extrapolation and two modeling approaches (Table 1) to estimate water, N, and P export from ungauged areas. The approaches were: (1) spatial extrapolation of the long-term observed yields (area-normalized) at the USGS gauging station, (2) hydrochemical modeling with local adjustments for human populations and land use only, and (3) hydrochemical modeling with parameter adjustments based on local characteristics.

These approaches varied from simple extrapolations (approach 1) to semi-distributed modeling (approach 3). In approach 1, we used the long-term observed yields at the USGS gauging station (Fisher et al. 1998) to extrapolate over ungauged areas, with no simulation modeling. This approach assumes that the gauged sub-basin is a representative sample of the Choptank basin, and we used the observed measurements of export from the gauged sub-basin to estimate whole basin export, as in Fisher et al. (1992) and Staver et al. (1996). In approach 2, we used the hydrochemical model GWLF to estimate export from ungauged areas, but we adjusted only the fundamental watershed information on land use areas and human populations. GWLF was calibrated in the gauged sub-basin (Lee et al. 2000), and in approach 2 we used the model parameters calibrated within the gauged sub-basin for all ungauged sub-basins. In approach 3, we adjusted not only the fundamental watershed information but also model parameters dependent on local conditions (see Table 1). The results of the three approaches were compared with observed or estimated export in order to estimate the importance of local

Table 1. Summary of the three approaches used to estimate nutrient export from ungauged areas of the Choptank basin. For each approach, the adjustments to parameters are listed, along with the basis for the adjustments

Approach	Summary	Parameters adjusted	Basis
1	spatial extrapolations of observed area-normalized yields	none	sub-basin areas
2	spatial modeling with GWLF	land use areas	GIS coverages
		population sizes	census data
3	spatial modeling (GWLF) with local adjustments	land use areas	GIS coverages
		population sizes	census data
		baseflow recession coefficient	sub-basin areas
		curve number for stormflow	land use, soil drainage properties
		N concentrations in groundwater	land use, hydric soils
		N concentrations in storm flow from agriculture	land use

conditions in determining fluxes from ungauged areas and to evaluate the errors of spatial extrapolations.

The hydrochemical model

We used a visual basic (VB) version of GWLF (Generalized Watershed Loading Functions, Lee et al. 2000) derived from the original model developed by Haith et al. (1992). This is a lumped parameter model that quickly and efficiently estimates monthly export of water, sediment, N, and P from a defined area; model input requirements are daily temperature and precipitation, land use, human populations, soil drainage characteristics, and agricultural cropping practices. The enhanced VB version of GWLF enabled us to interface the model to the Arc Macro Language for execution of ArcInfo commands within GWLF to access land use and soil data in order to calculate storm flow for each land use using the SCS curve number method.

We have previously calibrated and validated GWLF in the gauged sub-basin of the Choptank (Lee et al. 2000). At the annual time scale, the model produced relatively small errors for export of water, N, and P (10–50%), and local adjustments of watershed characteristics were essential to reproduce accurate water yields and nutrient export. There were two important model parameters that we adjusted locally: the groundwater recession coefficient (r, d^{-1}) and N concentrations, [N], in storm flow from agricultural land (mg L^{-1} or μM). The adjustment of r was based on an empirical relationship showing an inverse correlation between recession coefficients and watershed size (Lee et al. 2000). The adjustment of [N] in storm flow from agricultural land was based on a second empirical relationship showing an exponential relationship between agricultural land use and stream TN in the Choptank basin (Norton & Fisher 2000; Lee et al. 2000). Application of this empirical relationship was used to correct the linear assumption of GWLF. In this study, we introduce an additional local adjustment for [N] in groundwater based on hydric soil proportions (described below).

Subdivision of ungauged areas of the watershed

GWLF is a lumped parameter model using average basin characteristics to estimate export. To provide spatial information on export, we subdivided ungauged areas of the Choptank into 21 sub-basins, in addition to the gauged sub-basin (Figure 1, Table 2). We manually digitized the sub-basin boundaries on the basis of tidal and non-tidal stream segments, hydrogeomorphic regions (Hamilton et al. 1993), soil types (Norton & Fisher 2000), and water quality monitoring stations (Jordan et al. 1997; Norton & Fisher 2000). The 22 sub-basins cover the land area and allow us to estimate spatial variations

Table 2. Local characteristics of sub-basins within the Choptank River basin. Columns 1–6 were directly extracted from GIS data layers, whereas columns 7–14 represent parameter adjustments based on local characteristics and empirical relationships (Lee et al. 2000 & Figure 3). The sediment delivery ratio (column 7) was computed for each sub-basin using the empirical relationship between watershed sediment delivery and watershed areas (Haith et al. 1992; Novotny & Olem 1994). Groundwater recession coefficients (column 8) were calculated using an empirical relationship based on drainage areas (Lee et al. 2000); the value of 1 was assumed for areas <1 km^2. NO_3^- in groundwater (column 9) was the spatial average for each sub-basin using concentrations reported for land uses (Hamilton et al. 1993). Transfer coefficients (column 10) represent the fractional delivery of groundwater NO_3 calculated using an empirical relationship with hydric soils (Figure 3). Baseflow N (groundwater N delived to streams, column 11) was estimated by multiplying column 9 and 10. Population served by sewage systems (column 12) was obtained by intersecting the population coverage with the WWTP service areas (see Figure 1). Enhancement factors for stormflow N from agricultural land were computed from an exponential relationship between % agricultural land use and TN (Lee et al. 2000). Column 14 represents N concentrations in stormflow from agricultural land use based on the calibrated value in the gauged area (2.18 mg L^{-1} marked by *) multiplied by column (13). NA = not applicable

Sub-basin name		Local characteristics						Adjustments based on local characteristics							
	column	(1)	(2)	(3)	(4)	(5)	(6)	(7)	(8)	(9)	(10)	(11)	(12)	(13)	(14)
		km^2	%	%	%	%	1990	deliv.	recess.	mg L^{-1}	trans.	mg L^{-1}	sewered	enhance.	agri.
		Area	Agri.	Forest	Devel.	Hydric	Popul.	ratio	coeff.	$GWNO_3$	coeff.	BF NO_3	Popul.	factor	SF N
Bolingbroke Island		0.07	0	100	0	0.0	0	0.40	1.00	0.10	0.86	0.09	0	1.00	NA
Bolingbroke Creek		43.11	61	37	3	20.4	720	0.15	0.07	5.19	0.68	3.52	0	1.55	3.38
Broad Creek		49.02	56	35	9	50.3	2393	0.15	0.07	5.25	0.41	2.17	0	1.30	2.83
Cambridge		49.45	48	31	22	0.0	13102	0.15	0.07	5.47	0.86	4.70	12023	1.04	2.27
ChopTuck Junction		11.69	65	31	4	18.3	351	0.19	0.14	5.67	0.70	3.95	0	1.79	3.90
Gauged area		294.12	49	46	5	63.2	10531	0.08	0.05	4.41	0.30	1.31	334	1.00	2.18*
Gravelly Branch		45.32	68	32	0	48.9	555	0.16	0.07	5.61	0.42	2.38	0	2.06	4.49
Hambleton Island N		0.05	0	100	0	0.0	0	0.40	1.00	0.10	0.86	0.09	0	1.00	NA

Table 2. Continued

Sub-basin Name	Local characteristics						Adjustments based on local characteristics							
column	(1)	(2)	(3)	(4)	(5)	(6)	(7)	(8)	(9)	(10)	(11)	(12)	(13)	(14)
	km^2	%	%	%	%	1990	deliv.	recess.	mg L^{-1}	trans.	mg L^{-1}	sewered	enhance.	agri.
	Area	Agri.	Forest	Devel.	Hydric	Popul.	ratio	coeff.	$GWNO_3$	coeff.	BF NO_3	Popul.	factor	SF N
Hambleton Island	0.15	0	100	0	0.0	0	0.40	1.00	0.10	0.86	0.09	0	1.00	NA
Harris Creek	31.23	62	32	7	25.7	1131	0.18	0.08	5.56	0.63	3.51	0	1.63	3.55
Island Creek	55.07	67	29	4	40.0	1652	0.15	0.07	5.81	0.50	2.93	582	2.03	4.42
Knapps Island	0.06	0	100	0	0.0	11	0.40	1.00	0.10	0.86	0.09	0	1.00	NA
Oldtown Branch	24.95	67	31	2	51.2	310	0.18	0.09	5.69	0.40	2.30	0	2.02	4.40
Oligo Choptank W	145.02	66	32	2	15.1	2584	0.12	0.05	5.59	0.73	4.06	0	1.93	4.21
Oligo Choptank E	224.10	63	32	3	19.2	5900	0.09	0.05	5.79	0.69	3.99	355	1.61	3.51
Reeds Creek Marsh	0.16	0	100	0	0.0	0	0.40	1.00	0.10	0.86	0.09	0	1.00	NA
Secretary	75.56	61	33	6	1.5	3559	0.14	0.06	5.43	0.85	4.59	406	1.46	3.18
Tidal Fresh Choptank	216.53	59	33	9	27.6	10194	0.09	0.05	5.47	0.61	3.36	2993	1.42	3.10
Tidal Fresh Tuckahoe	169.24	75	22	3	20.4	3665	0.11	0.05	6.38	0.68	4.33	843	2.59	5.65
Tilghman Island	5.91	51	24	25	27.2	734	0.27	0.23	5.98	0.62	3.69	0	1.09	2.39
Tred Avon River	95.31	55	27	18	36.1	12389	0.13	0.06	5.80	0.54	3.12	9189	1.27	2.76
Upper Tuckahoe	219.63	71	28	1	46.6	2396	0.09	0.05	5.92	0.44	2.64	0	2.29	4.98
Land Total	1755.73	61	33	5	28.6	72177	NA	NA	NA	NA	NA	26725	NA	NA
Estuary	280.29	NA	NA	NA	NA	NA	NA	NA	NA	NA	NA	NA	NA	NA
Total Basin	2036.02	52	26	5	28.9	72177	NA	NA	NA	NA	NA	26725	NA	NA

in terrestrial diffuse sources of N and P. These sub-basins are larger than and include those defined in Norton and Fisher (2000) for the upper Choptank.

Compilation of Arc/Info coverages

Digital GIS data (watershed boundaries, soil, and land use) with a common projection (UTM) and datum (NAD27) were available from Mayers (1998) and Norton and Fisher (2000). The original coverage for land use contained a modified Anderson level 2 classification (Anderson et al. 1976). For modeling purposes, land uses were aggregated in two ways. To estimate nitrate concentrations ($[NO_3]$) in groundwater (described below), we aggregated land use into three groups: agriculture (cropland + feedlots + pasture), forest (all forest types + wetland), and developed (urban and suburban). To compute the SCS curve numbers for storm flow within GWLF, we maintained six simplified categories of land uses (agriculture, forest, feedlots, urban, and wetland), each with 4 types of soil drainage classes (A, B, C, and D). Soil coverages contained the USDA hydrologic soil drainage classes – A (well drained), B (moderately well drained), C (moderately poorly drained), and D (poorly drained), with an attribute of potentially hydric soils for classes C and D (USDA 1975, 1994).

Information on human populations (1990) was obtained from the Consortium for International Earth Science Information Network (CIESIN; ftp://ftp.ciesi.org/pub/census/usa/stf). The data were used to generate a point GIS coverage for human populations, and digitized sub-basin boundaries (Figure 1) were used to confine the point attribute data to estimate the 1990 population size within each sub-basin. Except for populations within or near towns served by a waste water treatment plant (WWTP), populations were assumed to be served by home septic systems and modeled accordingly by GWLF. To segregate populations served by waste water treatment plants from the total population, we digitized boundaries of the sewer pipelines, which were obtained from local waste water treatment plants (Easton and Cambridge, Table 3) or interpreted from county and USGS 7.5' maps for the remaining 9 stations (Figure 1, Table 3). Measured inputs from WWTPs associated with sewer pipeline boundaries (Fisher et al. unpub; A. Gutierrez, MD Dept. of Environment, pers. com.) were included as separate point sources.

*Base flow recession coefficient (*r*)*

The base flow recession coefficient (r, d^{-1}) describes the exponential rate at which base flow declines following a storm event. To estimate r for the ungauged sub-basins where flow measurements are not available, we used an inverse, empirical relationship between r and basin area (km^2), described

Table 3. Waste water treatment plants (WWTPs) within the Choptank River basin (see Figure 1). Data were compiled from Fisher (unpub.), Walters (1990), EPA Chesapeake Bay Program (http:/cobia.chesapeakebay.net/point_source/facility.cfm), and MD DNR (A. Gutierrez, pers. com.). Population data for 1990 was obtained from (ftp://ftp.ciesi.org/pu/census/usa/stf). MGD = millions of gallons per day (original units, converted to millions of liters per day for use here)

WWTP name	dd mm ss N latitude	dd mm ss W longitude	Sewered population	km^2 collection area	MGD average discharge	10^6 L d^{-1} average discharge	Mg N y^{-1} average TN flux	Mg P y^{-1} average TP flux
Cambridge	38°34′09″	–76°03′22″	12023	14.10	3.383	12.8	55.7 ± 2.8	16.33 ± 1.03
Denton	38°52′04″	–75°50′29″	2066	1.37	0.408	1.54	5.0 ± 1.8	1.79 ± 0.61
Easton	38°44′54″	–76°00′28″	8551	17.70	1.417	5.36	23.1 ± 2.3	6.95 ± 0.54
Greensboro	38°58′41″	–75°48′00″	826	1.00	0.132	0.50	2.7 ± 0.2	0.74 ± 0.05
N Caroline High	38°54′39″	–75°50′17″	101	0.01	0.002	0.01	0.1 ± 0.0	0.02 ± 0.01
Oxford	38°41′05″	–76°10′13″	638	0.92	0.075	0.28	0.7 ± 0.1	0.46 ± 0.06
Preston	38°42′24″	–75°54′19″	355	0.95	0.113	0.43	2.6 ± 0.3	0.39 ± 0.05
Ridgely	38°57′54″	–75°53′06″	843	1.26	0.109	0.41	3.7 ± 0.3	0.52 ± 0.06
Trappe	38°39′37″	–76°04′18″	582	0.83	0.100	0.38	1.4 ± 0.2	0.32 ± 0.04
Twin Cities	38°36′41″	–75°57′55″	406	1.04	0.217	0.82	3.0 ± 0.3	0.51 ± 0.05
Walker Trailer Park	39°06′19″	–75°45′23″	334	1.37	0.024	0.09	0.3 ± 0.0	0.05 ± 0.00
Total			26725	40.55	5.980	22.62	98.2 ± 4.5	28.08 ± 0.94

by Lee et al. (2000). Since the base flow recession coefficient was poorly constrained for small drainages <1 km^2, we assumed that r has a value of 1 for these areas. This assumption is equivalent to enhanced base flow transport into streams draining areas <1 km^2 only during the day of a storm event.

N in storm flow from agricultural land use

[N] in storm flow from agricultural areas was based on an empirical, non-linear relationship between % agricultural land use and stream [N] in the Choptank basin (Lee et al. 2000). [NO_3] and [TN] in stream waters increased exponentially with increasing % agricultural land use, particularly when agriculture exceeded 50% of land use. The non-linearity appeared to be due to losses of N trapping zones as agriculture expanded into marginal areas. Application of this exponential relationship corrected the linear assumption of GWLF and significantly reduced cumulative and RMS errors of model output during validation (Lee et al. 2000). To implement this relationship, we used an enhancement factor for [N] in storm flow from agricultural areas:

$$\text{enhancement factor}_i = [TN]_i/[TN]_g \quad (1)$$

where $[TN]_i$ is stream total N in sub-basin i estimated by the empirical non-linear relationship with % agriculture, and $[TN]_g$ is the volume-weighted mean, observed TN in the gauged sub-basin (1.59 mg L^{-1} = 114 μM, Fisher et al. 1998). The enhancement factor represents the effect of the non-linear increase in TN by the varying amounts of agriculture within each sub-basin relative to the gauged area (Table 2, column 13). We applied the enhancement factor to adjust [N] in storm flow for agricultural areas in each ungauged sub-basin:

$$adj\ [N]_i = cal\ [N]_g\ {}^*\text{enhancement factor} \quad (2)$$

where *adj* $[N]_i$ is the adjusted dissolved [N] in storm flow from agricultural areas in sub-basin i (Table 1, column 14), and *cal* $[N]_g$ is the calibrated dissolved [N] in storm flow from agricultural areas in the gauged sub-basin (2.18 mg N L^{-1} = 156 μM). *adj* $[N]_i$ is our best estimate of dissolved N in storm flow from agricultural areas in sub-basins of varying size and agricultural activity.

NO_3 in groundwater

[N] in groundwater is related to the overlying land use and soils (Freeze & Cherry 1979; Hamilton et al. 1993). Fertilizers, manures, septic N, and natural N are transformed through soil processes to highly soluble NO_3 as

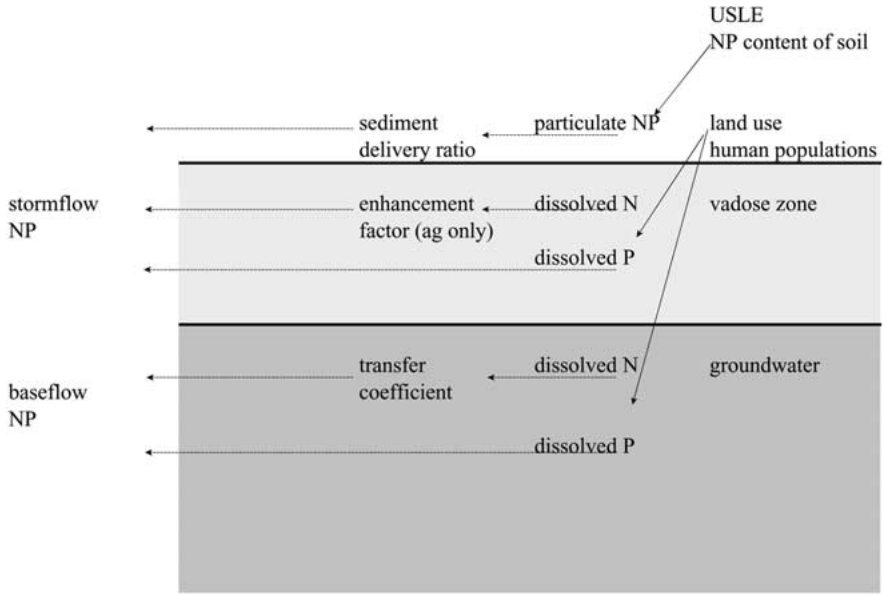

Figure 2. Conceptual model of the processes influencing the concentration of N and P in storm flow and base flow which are used by GWLF to model monthly export. Solid arrows represent effects on initial concentrations in soils, the vadose (unsaturated) zone, and in groundwater; dashed arrows represent flows in the soil layers and subsequent modification to concentrations based on empirical relationships known to be active on the landscape of the Choptank basin. The only adjustment to P concentrations is trapping of particulate P in floodplains and stream beds by the sediment delivery ratio, whereas N concentrations are increased by the non-linear effects of agriculture (enhancement factor, Eq. (1)) and reduced by particulate trapping (sediment delivery ratio) and by denitrification in hydric soils (transfer coefficient, Figure 3). USLE = Universal Soil Loss Equation, used by GWLF to estimate particulate mobilization in storm flow. Particulate transport is exclusively in the overland flow component of storm flow, whereas dissolved N and P transport occurs via overland flow and shallow through-flow (both computed as storm flow by GWLF).

water percolates through the vadose zone to groundwater (see Figure 2). NO_3 is the main form of N that occurs in groundwater (Freeze & Cherry 1979; McFarland 1996), and we used [NO_3] as a surrogate for total dissolved N in groundwaters.

On the Delmarva Peninsula, [NO_3] in shallow groundwaters (<15 m) is related to land use. Hamilton et al. (1993) reported [NO_3] as 0.1, 8.2, and 7.1 mg N L^{-1} (7.1, 586, and 507 μM) for forest, agriculture, and urban land uses, respectively, and we used these data to calculate the spatially averaged [NO_3] in groundwater (Table 2, column 9) based on the proportions of the three categories of aggregated land uses (Table 2, columns 2–4) for each of the 22 sub-basins as well as for the 34 non-tidal sub-basins defined in

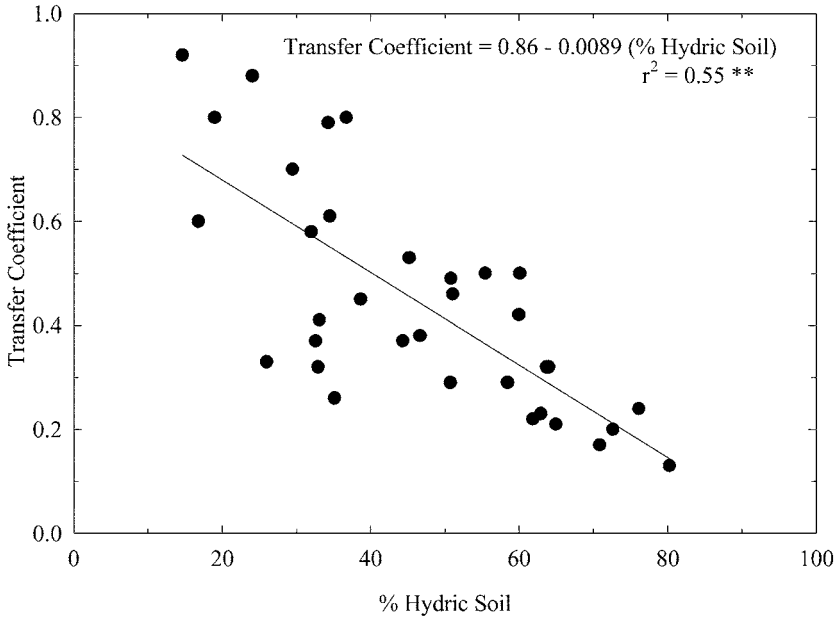

Figure 3. The relationship between % hydric soil and the transfer coefficient for nitrate from groundwater to streams in the Choptank basin. The transfer coefficient is defined as the fractional delivery of groundwater nitrate to streams (see Eq. (3) in text).

Norton and Fisher (2000). Within the latter sub-basins, the spatially averaged groundwater [NO_3] always exceeded the base flow stream [NO_3] observed by Norton and Fisher (2000), and we defined a transfer coefficient that accounts for losses of NO_3 between groundwater and base flow of the stream water:

$$\text{transfer coefficient} = \text{observed } [NO_3] \text{ in base flow} / \text{estimated } [NO_3] \text{ in groundwater} \quad (3)$$

We found that the transfer coefficients were significantly and inversely correlated with % hydric soils for the 34 non-tidal sub-basins of Norton and Fisher (2000). This relationship, shown in Figure 3, is probably the result of denitrification in hydric soils. We used this empirical relationship to estimate fractional N losses from groundwater in the 22 sub-basins of Figure 1 with varying land use and proportions of hydric soils (Table 2, column 10). The estimated groundwater [NO_3] (Table 2, column 9) was multiplied by the transfer coefficient (Table 2, column 10) to estimate [NO_3] delivered to streams in base flow (Table 1, column 11; Figure 2).

WWTP

We compiled monthly, average discharge records for 11 waste water treatment plants (WWTPs) in the Choptank basin. Monthly discharge and chemistry records from 8 WWTPs were obtained from the Chesapeake Bay Program (*http://cobia.chesapeakebay.net/point_source/facility.cfm*), and records from 1 WWTP (Walker Trailer Park) were obtained from MD Dept. of the Environment (A. Gutierrez, pers., com.). The two largest, Easton and Cambridge, have been monitored monthly since 1984 (Walters 1990; Fisher 1992, unpub.). These measurements were volume-weighted and transformed to Mg (10^6 g) N and P y^{-1}. The spatial locations of WWTPs are shown in Figure 1, and information for each plant is shown in Table 3.

Measurements of wet deposition

Atmospheric deposition to the water surface also contributes water, N, and P to the estuary of the Choptank. To estimate this diffuse source, we analyzed weekly precipitation obtained from two Aerochem Metrics Model 301 collectors at the National Atmospheric Deposition Program (NADP) MD 13 collection site at the Wye Research and Education Center (WREC), and from a site at Horn Point Laboratory (HPL, see Figure 1). Chemical analyses were performed on the unfiltered precipitation for total nitrogen (TN) and total phosphorus (TP) using the persulfate oxidation method of Valderrama et al. (1981). Briefly, duplicate 20 ml volumes were autoclaved in closed vials for 30 minutes with the oxidizing agent, and the resulting NO_3 and PO_4 were measured colorimetrically. NO_3 was measured by autoanalyser (Technicon AutoAnalyser 2), and PO_4 was manually measured using the method of Parsons et al. (1984).

Statistics

Linear regressions, correlations, and t tests were used for examining the significance of relationships or differences. The significance of the tests is indicated below as 'not significant' (NS, $p > 0.10$), 'marginally significant' (MS, $0.10 > p > 0.05$), 'significant' (*, $0.01 < p < 0.05$), or 'highly significant' (**, $p < 0.01$).

Results

Sub-basin descriptions

The Choptank basin is a rural area dominated by agriculture and forest. The areas of sub-basins shown in Figure 1 ranged from <1 km^2 for some islands to 294 km^2 for the sub-basin gauged by USGS (Table 2, column 1). Except for small forested islands, most of the sub-basins had a mixture of land uses dominated by agriculture, ranging from 48% in the Cambridge sub-basin to 75% in the Tidal Fresh Tuckahoe sub-basin (Figure 1, Table 2, column 2). Forest land cover ranged from 22% in the Tidal Fresh Tuckahoe to 100% on some small islands (Figure 1, Table 1, column 3). Urban land use was 1% in the Upper Tuckahoe sub-basin, increasing to 25% at Tilghman Island (Table 2, column 4).

Model adjustments for sub-basins

Base flow recession coefficients

The area of each sub-basin determined the value of the groundwater recession coefficient (r, Lee et al. 2000). This coefficient describes the exponential drop in stream flow following a storm, and for ungauged sub-basins estimates of r ranged from 0.046 to 1 (Table 1, column 8). Most sub-basins having drainage areas similar to the gauged watershed had recession coefficients of 0.05–0.07, similar to the optimized value obtained during calibration of the gauged watershed (0.05) by Lee et al. (2000).

% Agriculture corrections & associated storm flow N

We have previously shown that agricultural land use has exponential (not linear) effects on [N] in streams of the Choptank basins (Lee et al. 2000). We have parameterized this effect as an enhancement factor (Eq. (1)), which augments the calibrated value of dissolved N in storm flow from agricultural areas of the gauged basin (2.18 mg L^{-1} = 156 μM). Since all sub-basins except small forested islands had equivalent or greater amounts of agriculture compared to the gauged sub-basin, enhancement factors were as high as 2.59 for the highest agricultural land use (Table 2, column 13), reflecting the proportion of agricultural land within each sub-basin (Table 2, column 2), and correcting the linear assumption of GWLF for the observed exponential relationship in the Choptank basin (Lee et al. 2000; Norton & Fisher 2000). Estimated dissolved N from agricultural lands were 2–6 mg N L^{-1} (143–429 μM) for agricultural storm flow from sub-basins with more agriculture than the gauged sub-basin (Table 2, column 14).

[NO_3] in groundwater

The estimated, spatially averaged [NO_3] in shallow groundwater ranged from 0.1 to 6.4 mg L^{-1} (7–457 μM, Table 2, column 9), reflecting the proportions of overlying land uses (Table 2, column 2–4). For example, the Tidal Fresh Tuckahoe had relatively high estimated [NO_3] in groundwater (6.4 mg N L^{-1} = 457 μM) due to 75 % agricultural land use. Conversely, small sub-basins (e.g. Bolingbroke Island), in which forest was the only land cover, had estimated groundwater [NO_3] of 0.1 mg N L^{-1} (7 μM).

There are NO_3 losses as groundwater moves to streams, primarily due to denitrification (Peterjohn & Correll 1984; Simmons et al. 1992; McDowell et al. 1992; Hill 1996; Jordan et al. 1997). To parameterize this process in GWLF, we adjusted the groundwater [NO_3] using the transfer coefficient (Figure 3; Table 2, column 10) to correct for N losses associated with hydric soils (Table 2, column 5). The transfer coefficients ranged from 0.30 to 0.86 (Table 2, column 10), and the estimated base flow [NO_3^-] (Table 2, column 11) varied from 0.1 to 4.7 mg N L^{-1} (7–336 μM). When we used this approach to estimate [N] in groundwater delivered to base flow in the gauged basin, we obtained 1.31 mg N L^{-1} (94 μM), similar to the optimized value of 1.17 mg L^{-1} (84 μM) obtained during model calibration using 10 years of empirical data (Lee et al. 2000).

Sediment Delivery Ratio (SDR)

This dimensionless parameter was used to compute erosive soil loss of particulates from all sources (Figure 2). SDR is a ratio which represents the fraction of eroded soil that leaves a basin in stream flow (Novotny & Olem 1994) and is analogous to the nitrate transfer coefficient shown in Figure 3. Like the recession coefficient, the SDR exponentially decreases with watershed size due to flood plain and streambed trapping of particulates (Wischmeier & Smith 1978; Haith & Shoemaker 1987; Haith et al. 1992; Novotny & Olem 1994). SDR values for the Choptank sub-basins ranged from 0.08 to 0.4 (Table 2, column 7). Small forested islands had relatively large values (0.40), resulting in more efficient delivery of eroded sediments, although erosion from forests is low. In contrast, larger sub-basins such as Oligohaline Choptank E, with a delivery ratio of 0.09, delivered a smaller fraction of eroded soil to the watershed outlet due to basin storage and retention in stream channels.

Population

We distinguished two human population groups in each sub-basin: those served by individual septic systems and those served by waste water treatment plants (Table 2, column 12). In 1990, both the Tred Avon River and Cambridge sub-basins had the largest populations (>12,000, Table 2) due to

urbanization (towns of Easton and Cambridge, Figure 1). Excluding small islands, populations for the remaining sub-basins ranged from 310 to 11,000, depending upon the size of the watershed. The total human population was 72,177 on a land area of 1756 km^2 (37% sewered, 67% on septic), with an average population density of 41 km^{-2}.

Adjusted [N] and [P]

The average values of [N] and [P] used by GWLF for base flow and storm flow from each land use are shown in Figure 4. Feedlots exhibited the highest modeled concentrations, particularly in storm flow, whereas forests had the lowest concentrations. Particulate concentrations were a substantial fraction of the TP only in storm flow from agricultural and urban areas. N values used for storm flow from land uses other than agriculture (e.g. forest, developed) were identical to the calibrated values obtained in the gauged area (Lee et al. 2000), with no adjustments, whereas N values for agriculture were adjusted as described above. Dissolved P from all types of land use in base and storm flows were the values obtained during calibration in the gauged sub-basin, without adjustments, due to the lack of known empirical relationships for P comparable to those of N (e.g. Figure 3).

Extrapolation over ungauged areas

Approach 1: extrapolation using the long-term observed yields at the gauged watershed

The long term (WY1980–1990) export of water, total N, and total P observed from the gauged sub-basin (Fisher et al. 1998) was used to extrapolate over the ungauged sub-basins, making no local adjustments except sub-basin areas (Tables 4 and 5). Diffuse sources in the gauged sub-basin contributed 99.8% of total N and 99.9% of total P exported at the gauge. We therefore ignored the very small contribution of N and P from the single WWTP (Walker Trailer Park, Table 3) within the gauged sub-basin, and we used the water, N, and P export coefficients measured by Fisher et al. (1998) in the gauged basin (38 cm y^{-1}, 6.2 kg N ha^{-1} y^{-1} and 0.30 kg P ha^{-1} y^{-1}) to estimate diffuse source export from the 21 ungauged sub-basins using only sub-basin areas.

In this approach, we assumed that the gauged sub-basin adequately represents the entire Choptank basin. Therefore, the water budget for the entire basin (Table 4) was exactly equivalent to the stream flow observed by USGS and processes modeled by Lee et al. (2000) in the gauged sub-basin (evapotranspiration, deep seepage, storm flow, and base flow). Over the 17 water years, rain inputs averaged 112 cm y^{-1}, and the biggest loss was evapotranspiration (62 cm y^{-1}), followed by stream flow (38 cm y^{-1}), and deep seepage out of the basin (11 cm y^{-1}). Stream flow was further partitioned

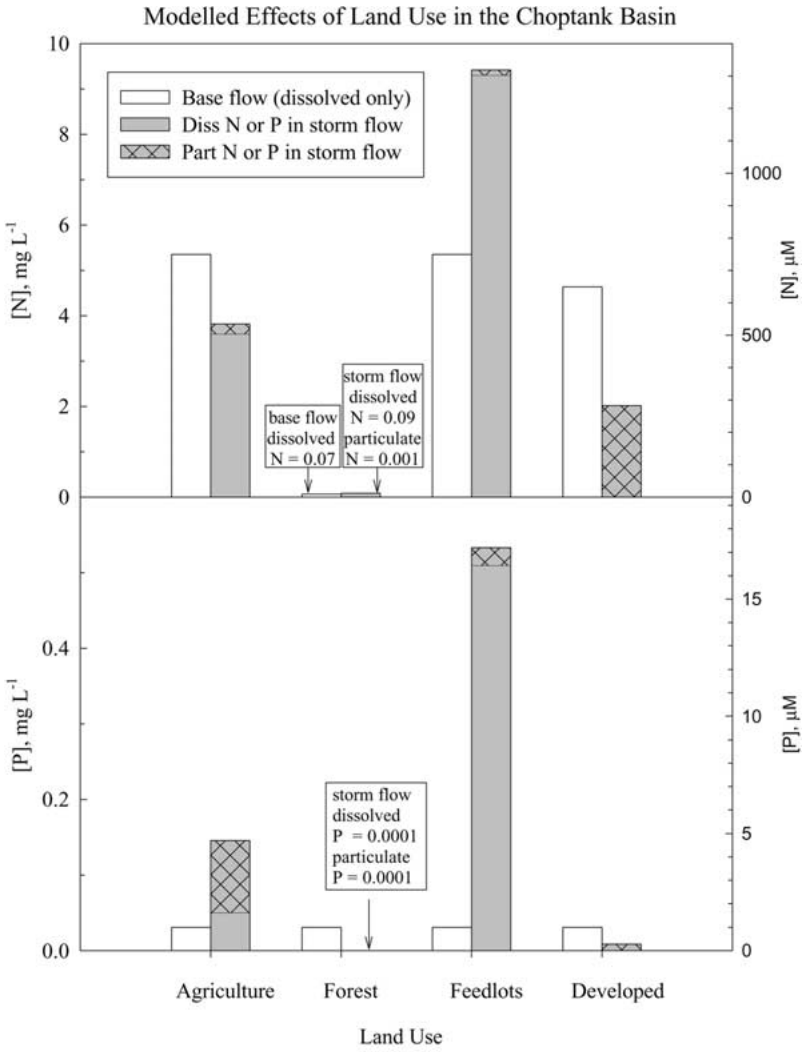

Figure 4. The average effects of land use on concentrations of N and P applied by GWLF to modeled base and storm flows. Concentrations were computed during WY1996 for the 17 largest polygons (those with all land uses and areas > 1 km^2). In general, concentrations were estimated as modeled, dissolved N and P output (Mg N or P), divided by modeled flow (m^3), with the following exceptions. The model assigns only dissolved loads to base flow for all land uses, whereas storm flow contains both dissolved and particulate N and P, except for developed areas, which contain only particulate loads in storm flows. Base flow concentrations of dissolved N were computed for each land use as the land use-specific groundwater N * average transfer coefficient computed for the 17 polygons on the basis of % hydric soils (Table 1, column 11). Concentrations of dissolved P in base flow were all 0.031 mg P L^{-1}, independent of land use. This value was obtained by optimization during model calibration (Lee et al. 2000). Storm flow dissolved N concentrations for agriculture were computed as the average value for storm N based on % agriculture in the 17 polygons (Table 2, column 14).

Table 4. Summary of annual water budgets for WY1980 to 1996 at the gauged sub-basin and for all sub-basins in the Choptank using the three approaches described in Table 1. Annual average rainfall was based on daily observations at 3 locations spanning the basin (Dover DE, Royal Oak MD, and Cambridge MD, see Figure 1); original data were reported in Lee et al. (2000). Streamflow in the gauged basin was measured by USGS, and storm flow and base flow were separated using modified USGS PART software (Lee et al. 2000). All other data were modeled. All units except drainage areas are in cm y^{-1}, and standard errors reflect interannual variations over 17 water years

Water Year 1980–1996	Gauged subasin	Approach 1 entire basin	Approach 2 entire basin	Approach 3 entire basin
drainage area (km^2)	293	1756	1756	1756
Rain	112 ± 5	112 ± 5	112 ± 5	112 ± 5
Water Budget				
(1) Evapotranspiration	62.1 ± 0.9	62.1 ± 0.9	61.9 ± 1.0	62.1 ± 1.0
(2) Deep Seepage	11.4 ± 0.9	11.4 ± 0.9	10.4 ± 0.9	9.8 ± 0.9
(3) Streamflow	38.5 ± 3.2	38.5 ± 3.2	39.7 ± 3.3	40.1 ± 3.3
stormflow	*11.1 ± 1.4*	*11.1 ± 1.4*	*14.4 ± 1.6*	*11.2 ± 1.2*
baseflow	*27.4 ± 2.3*	*27.4 ± 2.3*	*25.4 ± 2.2*	*28.9 ± 2.5*
SUM of 1, 2, 3	112 ± 5	112 ± 5	112 ± 5	112 ± 5

into storm flow and base flow (11 and 27 cm y^{-1}, Table 4). Because approach 1 was based on the observed N and P export coefficients measured in the gauged sub-basin, annual export of N and P was related only to the areas of the ungauged sub-basins. That is, small sub-basins contributed linearly less N and P than larger sub-basins (Table 5). Adding the estimated inputs from ungauged areas (excluding the nested sub-basins) with the measured values from the gauged area, the average annual export of TN and TP from terrestrial diffuse sources for the Choptank basin was 1085 Mg N y^{-1} and 53.6 Mg P y^{-1} (Table 5, approach 1).

Approach 2: modeling using GWLF with no local adjustments of parameters
In this approach, GWLF was used to perform simulations for each sub-basin during WY1980 to 1996, using the parameters of GWLF calibrated at the gauged site. We made local basin adjustments only for fundamental watershed properties (population and land use areas), and we used the values for the recession coefficient, curve numbers, and concentrations of N and P in groundwater and overland flow obtained during calibration in the gauged sub-basin (Table 1).

In the 17 water year simulation, temporal variations in observed rainfall and modeled evapotranspiration resulted in significant variations in modeled stream flow. Modeled stream flow averaged 40 cm y^{-1} (Table 4), composed of 25 cm y^{-1} base flow and 14 cm y^{-1} storm flow, the latter of which was significantly greater than storm flow observed at the gauging station (Table 4). The higher storm flow obtained in approach 2 was the result of lower forest cover in the basin outside the gauged area and slightly less evapotranspiration (62 cm y^{-1}), base flow (25 cm y^{-1}), and deep seepage out of the basin (10 cm y^{-1}) compared to the values estimated in approach 1. However, other than storm flow, there were no significant differences between major components of the water budgets obtained using approaches 1 and 2.

Spatially, the average annual values of export of N and P modeled using approach 2 closely followed sub-basin areas ($r^2 \approx 0.9$). Unlike approach 1, in which export was estimated using sub-basin areas ($r^2 \equiv 1$), in approach 2 variations in human populations and land use between sub-basins resulted in small deviations from a strict dependence on area. TN export ranged from a low of <0.01 Mg N y^{-1} from small sub-basins to a high of 191 Mg N y^{-1} from the largest sub-basin (the gauged watershed), many of which differed significantly (+ and –) from export obtained using approach 1. However, total terrestrial diffuse sources obtained with approach 2 were 1096 Mg N y^{-1}, statistically indistinguishable from the estimate obtained using approach 1 (1085 Mg N y^{-1}). TP export from the sub-basins obtained with approach 2 ranged from a low of < 0.01 Mg P y^{-1} from small sub-basins to 6.71 Mg P y^{-1} from the gauged sub-basin, most of which were significantly less than export obtained using approach 1 because GWLF underestimates P export during high flow months (Lee et al. 2000). Total terrestrial diffuse sources of P using approach 2 was 28 Mg P y^{-1} (Table 5, approach 2), which was significantly less than the estimate obtained with approach 1 (54 Mg P y^{-1}). The export values modeled with approach 2 corresponded to export coefficients of <0.7 kg N and <0.07 kg P ha^{-1} y^{-1} for the small, forested islands to ~8 kg N ha^{-1} y^{-1} from urbanized sub-basins (e.g. Cambridge) and 0.52 kg P ha^{-1} y^{-1} from sub-basins with high agricultural land cover (e.g. German Branch).

Approach 3: modeling using GWLF with local parameter adjustments

In this approach GWLF performed simulations for each sub-basin in the entire Choptank watershed for WY1980 to WY1996, adjusting model parameters associated with local properties (Table 1, Figures 2–4). Over the 17 water years, the major components of the water budget (evapotranspiration, deep seepage, and stream flow) obtained with approach 3 were statistically indistinguishable from values obtained in approaches 1 and 2 (Table 4); however, the components of stream flow (base and storm flow) obtained using

Table 5. Summary of annual export of N and P from Choptank sub-basins. The first two columns are observed export of total N and P from sub-basins defined in Norton and Fisher (2000) for 1985–1986, 4 of which correspond with sub-basins used here, plus the nested sub-basins of Norwich Creek and German Branch (Figure 1). Export from German Branch was compiled from observed measurements of Jordan et al. (1997) from WY1991 to WY1995. The last 6 columns are modelled export of N and P for 1980–1996 using three approaches (Table 1). To estimate total terrestrial diffuse sources, export from all basins were summed, except for the nested sub-basins. To estimate total inputs to the estuary, modeled terrestrial diffuse sources were added to measured atmospheric deposition (water surfaces only) and measured inputs from waste water treatment plants. All units are in Mg y^{-1} (10^6 g y^{-1})

Polygon name	Obs.	Obs.	Modeling approach					
			1		2		3	
	N	P	N	P	N	P	N	P
Bolingbroke Island			<0.1 ± 0.0	<0.01 ± 0.00	<0.1 ± 0.0	<0.01 ± 0.00	<0.1 ± 0.0	<0.01 ± 0.0
Bolingbroke Creek			26.6 ± 3.9	1.32 ± 0.23	20.7 ± 1.6	0.53 ± 0.05	54.7 ± 4.6	0.64 ± 0.06
Broad Creek			30.3 ± 4.5	1.49 ± 0.26	37.6 ± 2.3	0.68 ± 0.06	58.6 ± 4.1	0.83 ± 0.08
Cambridge			28.3 ± 4.2	1.40 ± 0.24	36.8 ± 2.0	0.55 ± 0.05	74.4 ± 5.6	0.65 ± 0.06
ChopTuck Junction			7.2 ± 1.1	0.36 ± 0.06	6.9 ± 0.5	0.17 ± 0.02	17.8 ± 1.5	0.20 ± 0.02
Gauged area	191.8 ± 98.2	6.32 ± 3.16	181.8 ± 26.8	8.97 ± 1.56	190.7 ± 12.7	6.71 ± 0.39	190.4 ± 12.7	6.71 ± 0.39
Gravelly Branch	68.8 ± 1.1	1.11 ± 0.50	28.0 ± 4.1	1.38 ± 0.24	23.8 ± 1.9	0.67 ± 0.06	51.2 ± 4.3	0.82 ± 0.08
Hambleton Island N			<0.1 ± 0.0	<0.01 ± 0.00	<0.1 ± 0.0	<0.01 ± 0.00	<0.1 ± 0.0	<0.01 ± 0.00
Hambleton Island			0.1 ± 0.0	<0.01 ± 0.00	0.1 ± 0.0	<0.01 ± 0.00	<0.1 ± 0.0	<0.01 ± 0.00
Harris Creek			19.3 ± 2.8	0.95 ± 0.17	21.7 ± 1.5	0.44 ± 0.04	45.6 ± 3.5	0.53 ± 0.05
Island Creek			34.0 ± 5.0	1.68 ± 0.29	32.2 ± 2.4	0.77 ± 0.07	71.1 ± 5.7	0.92 ± 0.08
Knapps Island			<0.1 ± 0.0	<0.01 ± 0.00	<0.1 ± 0.0	<0.01 ± 0.00	<0.1 ± 0.0	<0.01 ± 0.00

Table 5. Continued

Polygon name	Obs.	Obs.	Modeling approach					
			1		2		3	
	N	P	N	P	N	P	N	P
Oldtown Branch	13.4 ± 6.0	0.20 ± 0.09	15.4 ± 2.3	0.76 ± 0.13	13.7 ± 1.1	0.36 ± 0.03	28.1 ± 2.3	0.47 ± 0.04
Oligohaline Choptank E			138.5 ± 20.4	6.84 ± 1.19	134.1 ± 9.8	3.33 ± 0.31	323.6 ± 26.1	3.02 ± 0.27
Oligohaline Choptank W			89.6 ± 13.2	4.42 ± 0.77	74.7 ± 6.0	1.99 ± 0.19	200.1 ± 17.0	2.04 ± 0.19
Reeds Creek Marsh			0.1 ± 0.0	<0.01 ± 0.00	<0.1 ± 0.0	<0.01 ± 0.00	<0.1 ± 0.0	<0.01 ± 0.00
Secretary			48.9 ± 7.2	2.42 ± 0.42	49.7 ± 3.2	0.95 ± 0.08	131.8 ± 10.4	1.12 ± 0.10
Tidal Fresh Tuckahoe			104.6 ± 15.4	5.16 ± 0.90	101.0 ± 7.7	2.66 ± 0.25	285.5 ± 23.4	2.62 ± 0.24
(Norwich Creek – nested)	34.9 ± 13.0	0.98 ± 0.53	15.1 ± 2.2	0.75 ± 0.13	12.8 ± 1.0	0.35 ± 0.03	35.9 ± 3.0	0.45 ± 0.04
Tidal Fresh Choptank			133.8 ± 19.7	6.60 ± 1.15	154.1 ± 9.8	3.07 ± 0.27	293.5 ± 21.7	2.93 ± 0.25
Tilghman Island			3.7 ± 0.5	0.18 ± 0.03	2.1 ± 0.2	0.10 ± 0.01	10.7 ± 0.7	0.10 ± 0.01
Tred Avon River			58.9 ± 8.7	2.91 ± 0.51	77.7 ± 4.3	1.21 ± 0.10	128.2 ± 8.8	1.36 ± 0.12
Upper Tuckahoe	293.9 ± 98.9	3.07 ± 1.02	135.7 ± 20.0	6.70 ± 1.16	118.9 ± 9.6	3.40 ± 0.31	264.5 ± 22.7	3.46 ± 0.32
(German Branch – nested)	87.7 ± 11.7	4.10 ± 0.61	29.0 ± 4.3	1.43 ± 0.25	29.8 ± 3.4	2.46 ± 0.36	99.5 ± 9.6	2.53 ± 0.36
Terrestrial diffuse sources (excluding nested sub-basins)			1085.0 ± 50.7	53.55 ± 2.95	1096.5 ± 24.4	27.59 ± 0.74	2230.0 ± 54.7	28.43 ± 0.73
Atmospheric deposition (on water only)			155.0 ± 16.5	1.08 ± 0.10	155.0 ± 16.5	1.08 ± 0.10	155.0 ± 16.5	1.08 ± 0.10
WWTP (Point sources on land)			98.2 ± 4.5	28.08 ± 0.94	98.2 ± 4.5	28.08 ± 0.94	98.2 ± 4.5	28.08 ± 0.94
Total inputs to estuary			1338.2 ± 53.5	82.71 ± 3.10	1349.7 ± 29.8	56.75 ± 1.20	2483.2 ± 57.3	57.59 ± 1.20

approach 3 differed significantly than those obtained using approach 2 (Table 4). The greater base flow and decreased storm flow resulted from greater proportions of well-drained soils in the sub-basins outside of the gauged area, resulting in more percolation to groundwater. In effect, greater permeability of better drained soils compensated for lower forest cover outside the gauged basin cover to restore base and storm flow estimated in approach 3 to values indistinguishable from those observed in the gauged sub-basin.

Spatially, the modeled N and P export from terrestrial diffuse sources generally followed sub-basin area. However, the relationship was weaker than in the other two modeling approaches ($r^2 \approx 0.8$) because of the influence of local characteristics on the model parameters. TN export ranged from a low of <0.1 Mg N y^{-1} from small sub-basins to 324 Mg N y^{-1} from Oligohaline Choptank E, and most of these were significantly greater than export obtained with either approaches 1 or 2 (Table 5). Unlike approaches 1 and 2, the gauged sub-basin, with the largest area, did not exhibit the highest value of N export. Instead, several smaller sub-basins had higher N export due to larger proportions of agriculture and well-drained soils (Table 2). Total terrestrial N export from diffuse sources was 2230 Mg N y^{-1} (Table 5, approach 3), which was significantly greater than obtained in approaches 1 and 2. The TP export modeled with approach 3 ranged from <0.01 Mg P y^{-1} for small sub-basins to 6.71 Mg P y^{-1} at the gauged watershed, many of which were significantly greater than obtained with approach 2, but significantly less than obtained with approach 1. As for approach 2, low export compared to approach 1 resulted from the lack of useful empirical relationships between P and sub-basin characteristics, as well as the tendency of GWLF to underestimate P export during high flows. Terrestrial diffuse sources of P obtained using approach 3 were 28.4 Mg P y^{-1} (Table 5, approach 3), not significantly different from approach 2 (27.6 Mg P y^{-1}), but significantly less than the extrapolated value for approach 1 (53.6 Mg P y^{-1}). The modeled export values in approach 3 corresponded to export coefficients <1 kg N and <0.07 kg P ha y^{-1} from small, forested islands to 21 kg N and 0.54 kg P ha^{-1} y^{-1} from the heavily agriculturalized German Branch sub-basin.

Other sources of N and P

Atmospheric deposition

We have estimated wet atmospheric deposition directly onto the estuarine water surface (280 km^2) using a 2-year record (1997–1999) of TN and TP within or near the Choptank River basin (Rochelle-Newall et al., sub.). These data indicate wet atmospheric deposition rates of 5.5 kg N and 0.027 kg P ha^{-1} y^{-1}. In addition, a 12-year record of observed measurements of dissolved inorganic N deposition (NH_4^+, NO_2^-, and NO_3^-) from a local NADP

site (Figure 1) indicated no significant trends for DIN deposition in this area, although there is large interannual variability in atmospheric deposition of DIN, primarily driven by interannual variations in rainfall. We have no available records of TN and TP for the period 1980–1996 since NADP measures only dissolved inorganic N. Therefore, we have assumed average values for TN and TP deposition from 1980 to 1996 using our 1997–1999 data. This resulted in additional diffuse source inputs from wet atmospheric N and P deposition directly to estuarine surfaces of 155 Mg N and 1.1 Mg P y^{-1} (Table 5).

WWTP input to the Choptank estuary

Total wastewater discharge into the Choptank from the 11 licensed plants averaged 23 $\times$ 10^6 L d^{-1} (Table 3). Although there are increasing volumes of discharge over time at most of the plants caused by population growth, [N] and [P] in the effluent have decreased due to improved plant management (e.g. overland flow treatment, settling ponds, and activated sludge). The result is that the flux of N and P (volume $\times$ concentration) has remained relatively stable during the period for which data are available (generally 1985 to 1999). This is particularly true in detailed records for the two largest plants, Cambridge and Easton (Fisher unpub.), which together discharge 80% of the total wastewater volume into the Choptank (Table 3). We have therefore used the average annual values for wastewater discharge of TN and TP from each plant in order to provide data for an average budget of N and P inputs to the estuary within the Choptank basin.

N and P flux from each plant was strongly related to the population served ($r^2 > 0.9$). Unit fluxes varied from 1–7 kg N and 0.1–1.4 kg P person-1 y^{-1}. For the entire basin, annual export of N and P from the 11 WWTPs summed to 98 Mg N and 28 Mg P y^{-1} (Table 3), equivalent to average values of 3.7 kg N and 1.0 kg P $person^{-1}$ y^{-1}, similar to values reported by others (Reckhow et al. 1980; US EPA 1980). The export sums from all plants in Table 3 have been used in Table 5 to estimate total inputs to the Choptank estuary for each modeling approach.

Discussion

Evaluation of the modeling approaches

Traditionally, area yield coefficients from gauged sites have been used to estimate nutrient export from nearby ungauged areas (e.g. Novonty & Olem 1994). Coastal plain basins in particular often require extrapolation over

areas much larger than the gauged sites (e.g. Figure 1), and hydrochemical models such as GWLF may provide a more accurate approach than area yield coefficients by modeling export using local properties. To explore this application of hydrochemical modeling, we compared the approaches outlined in Table 1 with observations to evaluate errors during estimation of export from ungauged sub-basins of the Choptank.

To evaluate each approach, we compared modeled results with two kinds of observations at annual time scales. The first set of observations was independent export data available for 1991–1996 from two gauged sub-basins: (1) monthly export based on daily stream flow and 1–2 grab samples per month taken by USGS from the gauged sub-basin (B. Majedi, pers. com.) and (2) monthly export based on weekly integrated stream flow and volume-integrated samples from a temporary gauge installed in German Branch (Jordan et al. 1997). Average annual export over 1991–1996 from these gauged sub-basins is shown in Table 5 as observed N and P export.

The second set of observations were from four ungauged sub-basins (Gravelly Branch, Oldtown Branch, Norwich Creek, Upper Tuckahoe). At these locations we estimated N and P export using a 14 month stream survey (2–4 samples per month) conducted in 1985–1986 (Norton & Fisher 2000). These sub-basins were chosen to span nearly the full range of sub-basin areas, from 25 to 294 km^2, since basin area was shown above to be one of the important determinants of basin export. To obtain estimated export from these ungauged sub-basins, values for the two overlapping months were averaged, and we combined the monthly averaged N and P concentrations with estimated average stream flow at the monthly time scale. The latter has been shown to be locally uniform on the Delmarva Pennsula to within 30% (Fisher 1992), which enabled us to use area-normalized discharge from the gauged sub-basin. Export from each of the four ungauged basins for each month (E_i, Mg $month^{-1}$) was estimated as:

$$E_i = [C]_i \ ^* \ Q'_g \ ^* \ A_i \ ^* \ 10^{-9} \tag{4}$$

where $[C]_i$ is the average concentration of TN or TP observed each month (mg L^{-1}) in sub-basin i, Q'_g is the long-term average stream flow for each month in the gauged sub-basin normalized per unit area (L km^{-2} $month^{-1}$), A_i is the area of ungauged sub-basin i (km^2), and 10^{-9} converts mg (10^{-3} g) to Mg (10^6 g). The annual export sums for each ungauged sub-basin are given in Table 5 as observed N and P export (Mg y^{-1}).

These two types of observed data on export (gauged sampling locations and ungauged stream surveys) are representive of data which might be available for validation of model results in other basins requiring extrapolation over large areas to obtain total basin diffuse source export. Neither type of

Table 6. Summary of the comparison of modeled and measured export from six sub-basins of the Choptank shown in Figure 5. The t statistic was used with the standard errors to test whether the intercepts were significantly different from 0 and 1, respectively (Y:$p > 0.05$, N:$p < 0.05$). Average % errors were computed as deviations between observed and modeled export for each approach and normalized to the observed value as a percentage

Approach	Element	r^2	Intercept	= 0?	Slope	= 1?	Ave.% error
1	N	0.74	0.79 ± 0.26	N	0.58 ± 0.17	N	43 ± 14
	P	0.63	0.11 ± 1.60	Y	1.22 ± 0.47	Y	92 ± 38
2	N	0.64	1.82 ± 3.09	Y	0.55 ± 0.20	N	43 ± 13
	P	0.90	-0.35 ± 0.56	Y	1.02 ± 0.17	Y	40 ± 12
3	N	0.98	9.42 ± 8.55	Y	0.89 ± 0.06	Y	27 ± 17
	P	0.90	-0.22 ± 0.56	Y	1.00 ± 0.16	Y	45 ± 19

observation is without error and is much more restricted in temporal coverage than the model output. However, these observed, estimated values for export provide benchmarks to evaluate model errors quantitatively.

In Figure 5 we have plotted the modeled export of N and P against the observed values for the three modeling approaches used in the Choptank basin. For N export (Figure 5(A)), approach 1 significantly underestimated the observed values for 4 of the 6 sub-basins. The intercept of the regression line was significantly greater than zero, and the slope is $\sim$0.6, significantly less than the 1:1 line of perfect agreement (Table 6). This indicates a bias with approach 1 which results in an underestimate of N export. Approach 2 for N export was similar, except that the intercept was not significantly different from zero, and the slope was even less than with approach 1. Approach 3 gave the best agreement with the observations: most points fell near the 1:1 line, the intercept was equivalent to zero, and the slope was equivalent to 1 (Table 6). Most error bars (both observed and modeled using approach 3) overlapped the 1:1 line, and only 2 of the 6 pairs of data differed significantly (Oldtown and Gravelly Branch).

For P export, we obtained a different pattern (Figure 5(B)). Approach 1 values were generally elevated above the 1:1 line, although only 3 pairs were significantly different (Oldtown Branch, Upper Tuckahoe, German Branch). Due to scatter in the data, the intercept and slope were not different from 0 and 1, respectively (Table 6). Approaches 2 and 3 for P export gave nearly indistinguishable results, and 3 pairs of the 6 were significantly different from observations, as for approach 1. However, the magnitude of the differences were smaller and were more evenly spread between positive and negative in approaches 2 and 3. Both sets of data plotted close to the

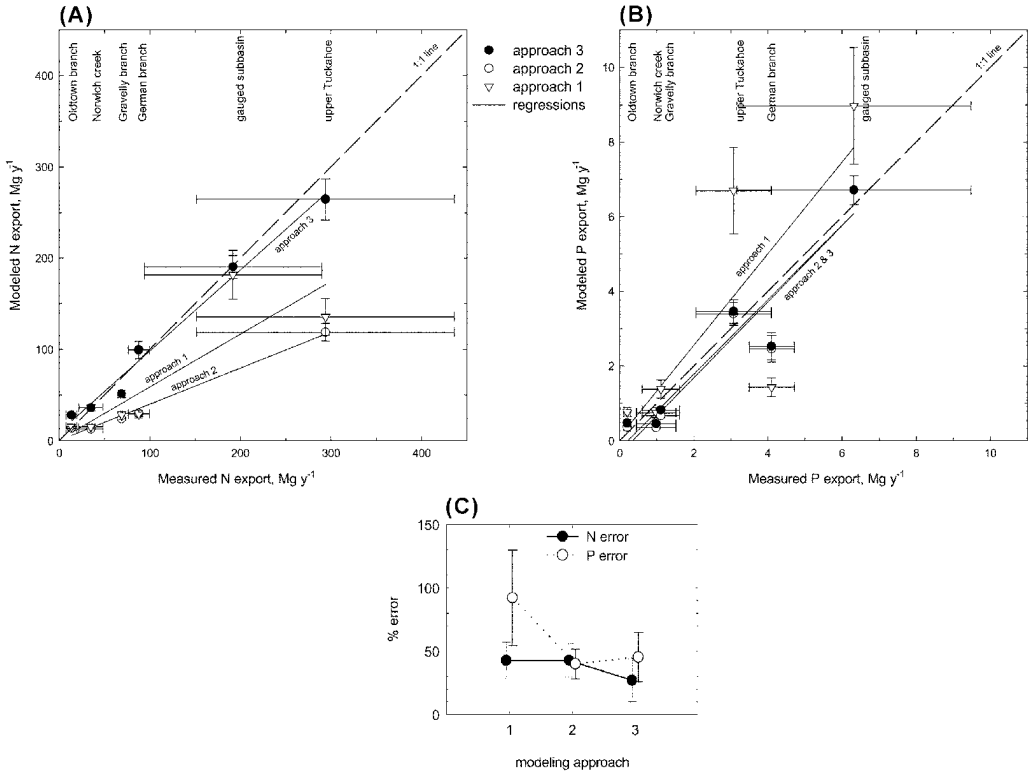

Figure 5. Comparison of measured export of N (panel A) and P (panel B) with modeled export estimated using the three approaches defined in Table 1. Statistics for the regression lines (solid lines) are given in Table 6. Error bars are standard errors of the means for WY1991–1996 resulting from interannual variations in rainfall. Panel C summarizes % errors (mean ± se) of the three approaches quantified as the deviations of the measured and modeled export values relative to the measured values.

1:1 line, with an intercept equivalent to zero, and a slope equivalent to 1 (Table 6). Statistically, there is little difference between the three approaches, except that the differences between modeled and observed were greater in approach 1.

We have used the data in Figures 5(A) and (B) to obtain the average errors expected with the three approaches. The size of the error bars in Figures 5(A) and 5(B) provides a visual estimate of the variability associated with the measurements and modeling as well as environmental variability (primarily annual rainfall). The absolute value of the differences between average observed and modeled export for each sub-basin was expressed as a percentage of the observed value, and the mean and standard error of these percent differences are shown in Figure 5(C) as a function of modeling approach. For N export, the errors associated with modeling approaches 1 and 2 (area yield coefficients and GWLF without local adjustments, respectively) were 40–50%, but declined to <30% for modeling approach 3 (GWLF with local adjustments). For P export, approach 1 resulted in errors >90% (factor of 2 uncertainty), whereas modeling approaches 2 and 3 both estimated export similarly, with errors of 40–50%.

This analysis shows that GWLF produced better estimates of export from ungauged areas than extrapolation of area yield coefficients. GWLF without local adjustments (approach 2) resulted in N export errors equivalent to those of yield coefficients (approach 1); however, the use of local adjustments (approach 3) significantly improved the ability of GWLF to predict observations of N export, reducing average errors from 43% to 27% (Figure 5(C)). Local adjustments had little effect on the ability to predict P export; however, the use of GWLF (with or without local adjustments) reduced P export errors from 92% to 40–45%. Since we had no empirical relationships with P parameters other than the SDR built into GWLF, this result was not surprising and suggests that improvements in GWLF may be achieved with empirical relationships between P concentrations and local characteristics, if any are found.

The errors using modeling approach 3 are nearly equivalent to the empirical errors in the observations. The stream flow values used to estimate export from the ungauged areas have errors of 10–30% at the monthly time scale (Fisher 1992), and errors associated with stream export (observations of stream flow and concentrations) are 7–25% (Cohn et al. 1992). The differences between modeled and observed export of N (27%) approach this range, whereas differences between modeled and observed P export (45%) exceed this range. Of the two, P export is more difficult to estimate because it is strongly associated with short-duration, high-flow events which are more difficult to sample than N export, which is dominated by

dissolved nitrate in base flow (Fisher et al. 1998). During calibration of GWLF in the gauged basin with a detailed, 11 year data set (daily stream flow, 10–20 water samples month^{-1}, Lee et al. 2000), we noted a tendency of GWLF to underestimate P export during high flow events; however, the modeled P export for 1991–1996 exceeded export estimates of USGS (Figure 5(B)), and export data from the 6 sub-basins in Figure 5(B) for approaches 2 and 3 show scatter but no significant bias for modeled P export (Table 6). We conclude that GWLF is an unbiased estimator of N and P export with errors of 27% and 45%, respectively, at the annual time scale.

It can be argued that there is some circularity in the comparisons described above. Initially, we calibrated (Lee et al. 2000) and adjusted the parameters of GWLF (this paper) using local observations such as those reported by Fisher et al. (1998), Norton and Fisher (2000), Jordan et al. (1997), and those shown in Figure 3. Then we compared the model output to a subset of the local observations spanning the range of sub-basin sizes. It may not be surprising, therefore, that the model's predictions of N export were more accurate with local adjustments. However, this was a test of the model's ability to incorporate and use local information to improve predictions compared to spatial extrapolation of area yield coefficients for N and P. If the model's performance had not improved, we would have concluded that hydrochemical modeling with GWLF was no better (and potentially worse) than spatial extrapolations from gauged sub-basins. Therefore, this was a true test of the model's ability to provide more accurate predictions (Figure 5(C)), and we conclude that GWLF with local adjustments (for N) or without local adjustments (for P) provides better estimates of export from ungauged areas with about half of the errors associated with spatial extrapolation of yield coefficients (Table 6). For other basins which require large extrapolations, the local adjustments applied to GWLF might differ from those used here, but our results indicate that the errors in the estimates of at least N export produced by GWLF should be less if local information is used to adjust the model parameters.

Approach 3 provided more accurate estimates of export because the adjustments were linked to known mechanisms of nutrient delivery. When we adjusted curve numbers using land use and soil drainage classes, GWLF generated less storm flow compared to approach 2 (Table 4) due to the larger proportions of well drained soil types A and B in the ungauged areas of the watershed (Lee et al. 2000). Further enhancing this effect, when we adjusted the base flow recession coefficients (Table 1) on the basis of watershed size, GWLF generated significantly more base flow than in approach 2 (Table 4). The greater base flow, plus the non-linear adjustment for high agricul-

tural land use (Lee et al. 2000), resulted in larger N export (Table 5), which more closely corresponded to observations (Figure 5(A)). When we adjusted the sediment delivery ratio using sub-basin areas, modeled export of P in approach 3 was marginally higher (MS, $p = 0.05$, see Figure 5(B)) than in approach 2 because of increased particulate P delivery in the ungauged sub-basins, all of which were smaller than the gauged sub-basin (Table 2). Each of these model adjustments was linked to known hydrologic mechanisms of nutrient delivery, and adjustments based on local characteristics improved model predictions, particularly for N export.

Test of the hypothesis

The hypothesis which we posed above was that area yield coefficients for N and P from ungauged areas would vary considerably from those of the gauged sub-basin due to spatial variations in land use, soils, and human populations. Using the data presented above for approach 3 (excluding forested islands), we found that the spatial variations in the area yield coefficients (export normalized per unit area of sub-basin) were 6–21 kg N and 0.13–0.54 kg P ha^{-1} y^{-1}. The highest N yields (15–25 kg ha^{-1} y^{-1}) were obtained using approach 3 for sub-basins with high agricultural (e.g. German Branch) or urbanized (e.g. Tilghman Island) land use (Figure 6(A)). Likewise, the highest P yields (0.4–0.6 kg P ha^{-1} y^{-1}) were estimated using approach 3 for sub-basins with large amounts of agriculture and/or poorly drained soils (e.g. German Branch, gauged sub-basin, Figure 6(B)). Excluding forested islands, N yields from sub-basins outside the gauged area were all higher than the gauged area, whereas P yields were higher in German Branch and lower elsewhere. These data clearly support the hypothesis that spatial variations in local conditions result in significant variations in yield coefficients. Excluding the forested islands, we estimated ~4 fold variations in area yield coefficients among sub-basins of the Choptank when we accounted for local characteristics (land use, soils, and human populations).

Inputs to the estuary

Terrestrial diffuse and point sources and wet atmospheric deposition of N and P to the Choptank estuary for WY1980–WY 1996 are summarized in Figure 7. Terrestrial diffuse sources, estimated using modeling approach 3, were the dominant N and P inputs to the estuary. TN from sewage outflows contributed only 4% of TN inputs to the estuary, but sewage TP contributed much more (49%). Wet atmospheric deposition directly onto the estuarine water surface corresponded to 6% of the TN and 2% of TP input from all sources. Because we used fixed land use and human population data for 1990, inputs of both

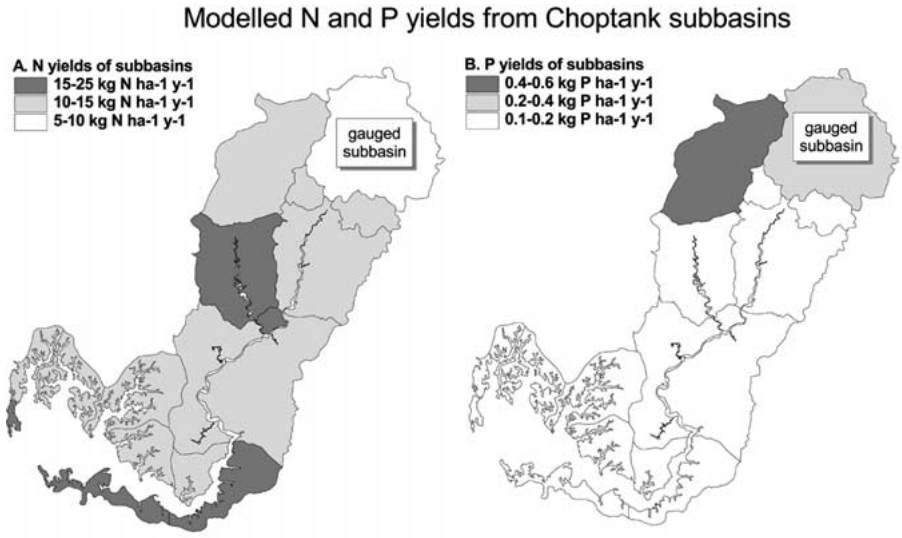

Figure 6. Spatial variations of annual N and P yields from Choptank sub-basins modelled by GWLF using approach 3. Yields were grouped into three classes for display purposes. See Figure 1 for location of the Choptank basin in the Mid-Atlantic region.

TN and TP from all known sources to the Choptank estuary exhibited no significant trends during WY 1980 to 1996, and the modeled annual inputs to the estuary from all known sources (point + terrestrial diffuse + atmospheric deposition = 2483 Mg N y^{-1} and 57.6 Mg P y^{-1}, Table 5) represent the long-term average for the 1980–1996 period. Neither dry atmospheric deposition nor inputs from exchange with Chesapeake Bay are included or known. The variability in the annual values in Table 5 is primarily due to the modeled effects of annual variations in rainfall, and changes in inputs to the estuary from anthropogenic effects such as changes in land use or populations are not included.

We have emphasized the annual time scale here for simplicity and because of the relevance to watershed management. However, data on shorter time scales illustrates the strong seasonal signals in terrestrial diffuse sources compared to the other known inputs (Figure 8). Average monthly inputs of TN to the Choptank estuary from all sources ranged over a factor of 5, from $\sim$70 Mg $month^{-1}$ in the low-flow summer months to $\sim$350 Mg $month^{-1}$ in high-flow spring months (Figure 8(A)). Although there was some seasonality in atmospheric and WWTP inputs of N, most of the monthly variation was due to the terrestrial diffuse sources. For all months, terrestrial diffuse sources contributed the largest proportion of TN inputs, similar to the long-term annual average, while inputs of TN from atmospheric deposition and WWTPs remained nearly uniform and contributed a maximum of only $\sim$30%

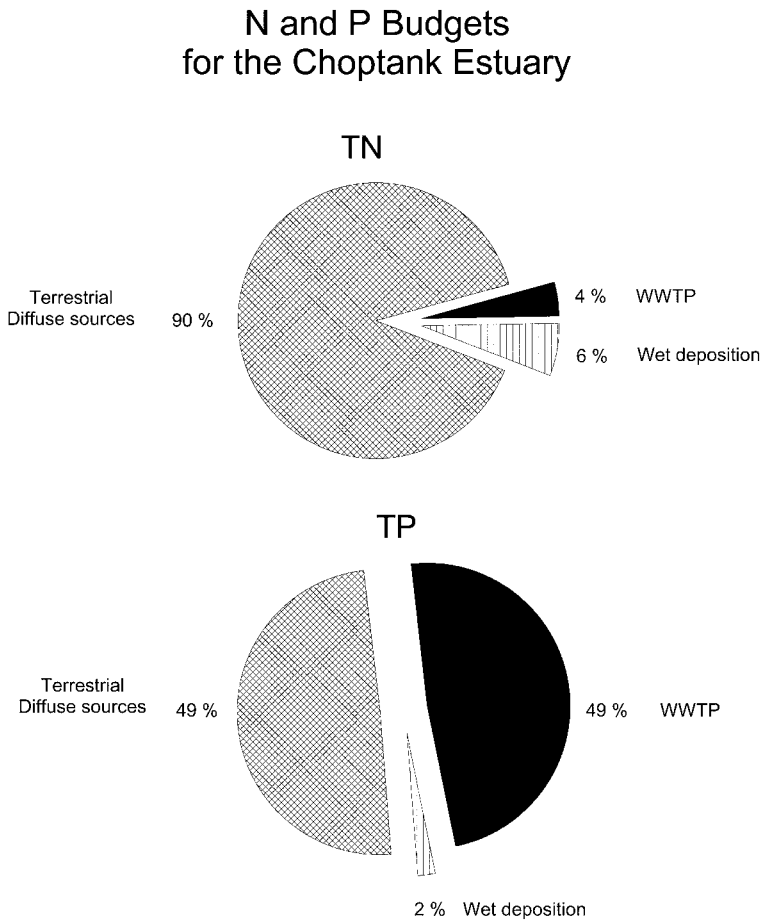

Figure 7. Annual summaries of the N and P input budgets to the Choptank estuary from terrestrial diffuse sources, WWTPs, and wet atmospheric deposition. Numerical values are given in Table 5.

during low flow months. Inputs of TP exhibited seasonal patterns similar to those of N (Figure 8(B)); however, TP varied only over a factor of 2, from ∼3 Mg month^{-1} to ∼6 Mg month^{-1}, buffered primarily by the high P content of inputs from WWTPs. Terrestrial sources and WWTPs contributed approximately equal amounts of P, while atmospheric deposition of P contributed only a small amount (almost invisible in Figure 8(B)).

The more damped seasonal cycle of P inputs resulted in annual variations in the N/P of the known inputs (Figure 8(C)). During the high flow months of winter and early spring, the molar ratio of inputs was ∼130:1, declining to ∼50:1 during the low flow months of late summer and early fall. Due to the

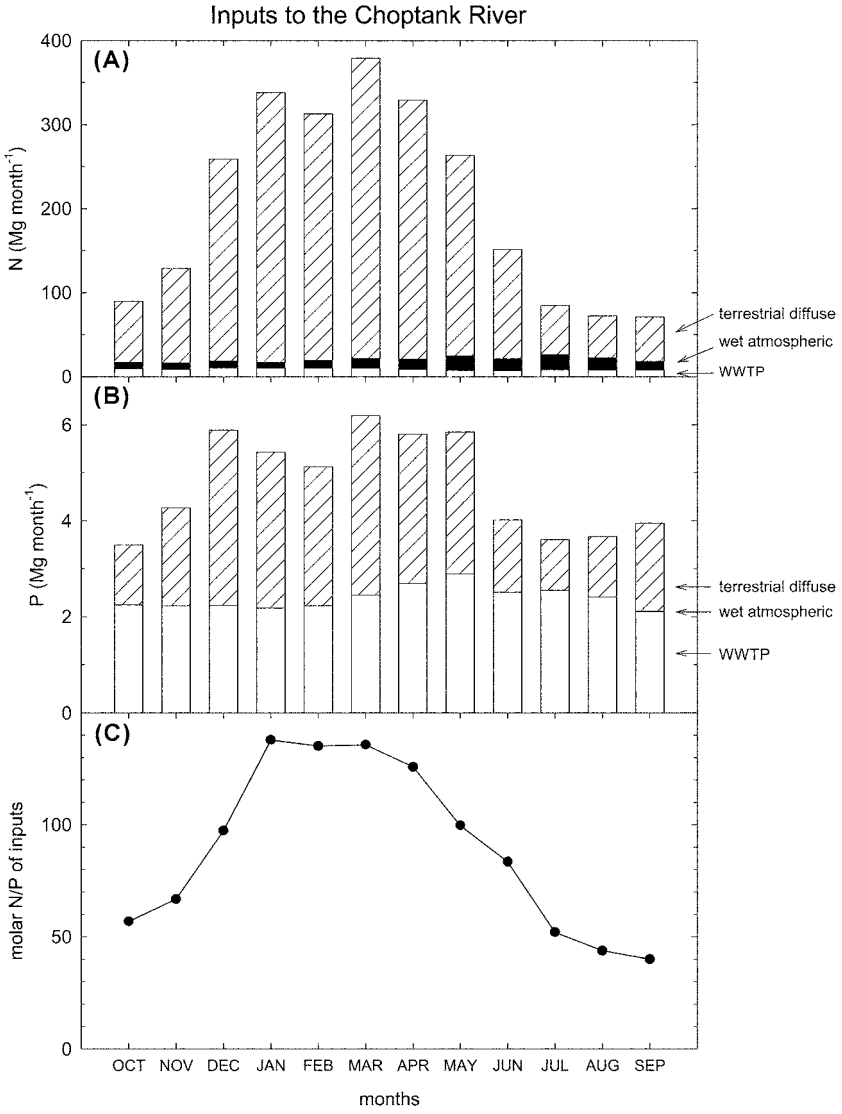

Figure 8. Monthly summaries of the average N and P inputs to the Choptank estuary (panels A and B), illustrating the large seasonal variations in N and P inputs from terrestrial diffuse sources. Panel C is the resulting seasonal variations in the molar N/P caused by the more damped seasonal signal of P inputs.

high retention of P by soils and high solubility of nitrate, terrestrial diffuse sources have high [N] but much smaller [P], with an average molar TN:TP of 101:1 (Fisher et al. 1998). The low P content of rainfall is due to the lack of significant gaseous forms of P, and wet atmospheric deposition resulted in large N inputs relative to P (molar TN:TP = 335:1). In contrast, WWTP inputs were highly enriched in P (molar TN:TP = 8:1) relative to the other known sources. The winter/spring inputs with high N:P appear to be the cause of the spring P limitation of algal growth and accumulation observed by Fisher et al. (1999) in the Choptank and other parts of Chesapeake Bay. Likewise, lower N inputs relative to P in summer appear to result in N limitation, although the molar N/P of inputs reported here exceed those of phytoplankton (16:1). However, differential losses of N and P occur within the aquatic system (e.g. marsh denitrification or particulate trapping) which are not included in GWLF.

There are clear management implications from this research. The data in Table 5 and Figures 7–8 provide considerable justification for advanced tertiary treatment of WWTP discharges for P removal. P from this source constituted approximately half of the inputs to the estuary, and reductions in wastewater P inputs could easily meet the EPA Bay Program's goal of 40% reductions. For instance, partial tertiary treatment installed at the Easton WWTP (a grassed, overland flow system) has reduced its N and P outflows by 33 and 57%, respectively, or 0.4% of all N sources and 10.9 % of all P sources (Fisher, unpub.). Although N inputs from WWTPs are small compared to the much larger contributions from terrestrial diffuse sources, efforts to reduce waste water P are likely to reduce N as well. However, N reductions should be focused on sources resulting from agriculture and home septic systems (production of food and disposal of human wastes). These are clearly the dominant sources of N that should be targeted to achieve 40% reductions in N inputs within this basin.

Acknowledgments

This research was partially supported by NASA MTPE (OES), US Fish and Wildlife Service, and the Electric Power Research Institute. We thank Brenda Majedi at USGS for N and P export data and Angelica Gutierrez and her research team at Maryland Department of the Environment for providing information on waste water treatment plants.

References

Anderson JR, Hardy EE, Roach JT & Witmer RE (1976) A land use and land cover classification system for use with remote sensor data. USGS Professional Paper 964. U.S. Government Printing Office, Washington, DC

Arnold Jr EJ, Bierbaum R, Chisholm C, Fox JC, Givens JD, Gonzalez IM, Groat C, Hampton J, Holstein E, Humiston G, Judge P, Kohnen A, Mahfood S, Martin P, Mayer G, Saunders S, Schiffer LJ, Studders K, Wheeler KD & Young JR (2001) Action plan for reducing, mitigating, and controlling hypoxia in the Northern Gulf of Mexico. US EPA Report: www.epa.gov/msbasin/ActionPlan.pdf

Beaulac MN & Reckhow KH (1982) An examination of land use – nutrient export relationships. Water Resour. Bull. 18(6): 1013–1024

Cohn TA, Culder DL, Gilroy EJ, Zynjuk LD & Summers RM (1992) The validity of a simple statistical model for estimating fluvial constituent loads: an empirical study involving nutrient loads entering Chesapeake Bay. Water Resour. Res. 28: 2353–2363

Cooper SR & Brush GS (1991) Long-term history of Chesapeake Bay anoxia. Science 254: 992–996

Fisher DC & Oppenheimer M (1991) Atmospheric nitrogen deposition and the Chesapeake Bay estuary. Ambio 23:102–208

Fisher TR (1992) Nutrient inputs to the Choptank River, Final report to US Fish and Wildlife Service (14-16-0005-8-9035)

Fisher TR, Lee K-Y, Berndt H, Benitez JA & Mayers Norton M (1998) Hydrology and chemistry of the Choptank river basin in the Chesapeake Bay drainage. Water, Air and Soil Pollution 105: 387–397

Fisher TR, Gustafson AB, Sellner K, Lacoutur R, Haas LW, Wetzel RL, Magnien R, Everitt D, Michaels B & Karrh R (1999) Spatial and temporal variation of resource limitation in Chesapeake Bay. Marine Biology 133: 763–778

Freeze RA & Cherry JA (1979) Groundwater. Prentice-Hall, Englewood Cliffs, NJ

Gardner RH, Castro MS, Morgan R & Seagle SW (1997) Nitrogen dynamics in forested lands of the Chesapeake basin: STAC Ches. Bay Prog. Ches. Res. Consort. Pub. 151, 36 pp

Haith DA & Shoemaker LL (1987) Generalized watershed loading functions for stream flow nutrients. Water Resour. Bull. 23(3): 471–478

Haith DA, Mandel R & Wu RS (1992) Generalized Watershed Loading Functions Version 2.0 User's Manual, Ithaca, Cornell University

Hamilton PA, Denver JM, Phillips PJ & Shedlock RJ (1993) Water-quality assessment of the Delmarva Peninsula, Delaware, Maryland, and Virginia-Effects of agricultural activities on, and distribution of, nitrate and other inorganic constituents in the surficial aquifer. US Geological Survey Open-File Report 93–40

Hill AR (1996) Nitrate removal in stream riparian zones. Journal of Environmental Quality 25: 473–755

Hopkinson CS Jr & Vallino JJ (1995) The relationships among man's activities I watersheds and estuaries: a model of runoff effects on patterns of estuarine community metabolism. Estuaries 18(4): 598–621

Jordan TE, Correll DL & Weller DE (1997) Effects of agriculture on discharges of nutrients from coastal plain watersheds of Chesapeake Bay. Jnl of Environ. Qual. 26: 836–848

Lee K-Y, Fisher TR, Jordan TE, Correll DL & Weller DE (2000) Modeling the hydrochemistry of the Choptank River basin using GWLF and Arc/Info: I. Model calibration and validation. Biogeochem. 49: 143–173

Linker L (1996) Models of the Chesapeake bay. Sea Technology 37(9): 49–55

Malone TC, Crocker LH, Pike SE & Wendler BW (1988) Influences of river flow on the dynamics of phytoplankton production in a partially stratified estuary. Mar. Ecol. Prog. Ser. 48: 235–249

Mayers M (1998) Land cover, soil properties, geomorphology and stream water quality in two coastal plain basins in the Chesapeake Bay water. Ph.D. Dissertation, University of Maryland, College Park

McDowell WH, Bowden WB & Asbury CE (1992) Riparian nitrogen dynamics in two geomorphologically distinct tropical forest watersheds: subsurface solute patterns. Biogeochem. 18: 53–75

McFarland ER (1996) Groundwater flow, geochemistry, and effects of agricultural practices on nitrogen transport at study sites in the Piedmont and coastal plain physiographic provinces, Patuxent River basin, Maryland. USGS Water Supply 2449

MD DNR (1996) Choptank River. Tributary Team Annual Report 1995–1996

Nixon SW (1987) Chesapeake Bay nutrient budgets – a reassessment. Biogeochem. 4: 77–90

Norton MM & Fisher TR (2000) The effects of forest on stream water quality in two coastal plain watersheds of the Chesapeake Bay. Ecological Engineering 14: 337–362

Novotny V & Olem H (1994) Water Quality. Prevention, Identification, and Management of Diffuse Pollution, Van Nostrand Reinhold, New York, 1054 pp

Officer CD, Lynch DR, Setlock GH & Helz GR (1984) Recent sedimentation rate in Chesapeake Bay. In: Kennedy (Ed.) The Estuary as a Filter (pp 131–157). Academic Press, New York

Orth RJ & Moore KA (1983) Chesapeake Bay: an unprecedented decline in submerged aquatic vegetation. Science 222: 51–52

Parsons TR, Maita Y & Lalli CM (1984) A Manual of Chemical and Biological Methods for Seawater Analysis, 1st edition, Pergamon Press, New York

Peierls BL, Caraco NF, Pace ML & Cole JJ (1990) River nitrogen export linked to human population density. Nature 350: 386–387

Peterjohn WT & Correll DL (1984) Nutrient dynamics in an agricultural watershed: observation on the role of a riparian forest. Ecology 65(5): 1466–1475

Reckhow KH, Beaulac MN & Simpson JT (1980) Modeling phosphorus loading and lake response under uncertainty: a manual and compilation of export coefficients. EPA Rep. 440/5-80-011

Rochelle-Newall EJ, Fisher TR & Radcliffe G (in review) Wet deposition of atmospheric CNP on a Delmarva coastal plain basin. Atmos. Environ.

Seliger HH, Boggs JA & Biggley WH (1985) Catastrophic anoxia in the Chesapeake Bay in 1984. Science 228: 70–73

Simmons RC, Gold AJ & Groffman PM (1992) Nitrate dynamics in riparian forests: groundwater studies. Journal of Environmental Quality 21: 659–665

Staver LW, Staver KW & Stevenson JC (1996) Nutrient inputs to the Choptank River estuary: implications for watershed management. Estuaries 19: 243–358

Stevenson JC, Staver LW & Staver KW (1993) Water quality associated with survival of submersed aquatic vegetation along an estuarine gradient. Estuaries 16(2): 346–361

USDA Soil Conservation Service (1975) Soil Taxonomy: A basic system of soil classification for making and interpreting soil surveys. USDA Soil Conservation Service, Agric. Hdbk. 436, Jon Wiley and Sons, NY, 754 pp

USDA Soil Conservation Service (1994) National Food Security Act manual. Title 180. USDA Soil Conservation Service, Washington, DC

US EPA (1980) Design manual: onsite wastewater treatment and disposal systems. Off. Water Prog. Oper. Wash. DC, EPA Rep. 625/1-80-012

Valderrama JC (1981) The simultaneous analysis of total nitrogen and total phosphorus in natural waters. Marine Chemistry 10: 109–122

Walters CP (1990) Nutrient inputs to the Choptank River. MS Thesis, University of Maryland, 99 pp

Wischmeier WH & Smith DD (1978) Predicting rainfall erosion losses – a guide to conservation planning. USDA, Agriculture Handbook No. 537